

CrossMark  
click for updatesCite this: *Chem. Sci.*, 2015, **6**, 7293

## Multistep energy and electron transfer processes in novel rotaxane donor–acceptor hybrids generating microsecond-lived charge separated states†

Sabrina V. Kirner,<sup>a</sup> Christian Henkel,<sup>a</sup> Dirk M. Guldi,<sup>\*a</sup> Jackson D. Megiatto Jr,<sup>‡b</sup> and David I. Schuster<sup>\*b</sup>

A new set of  $[\text{Cu}(\text{phen})_2]^+$  based rotaxanes, featuring [60]-fullerene as an electron acceptor and a variety of electron donating moieties, namely zinc porphyrin (ZnP), zinc phthalocyanine (ZnPc) and ferrocene (Fc), has been synthesized and fully characterized with respect to electrochemical and photophysical properties. The assembly of the rotaxanes has been achieved using a slight variation of our previously reported synthetic strategy that combines the Cu(i)-catalyzed azide–alkyne cycloaddition reaction (the “click” or CuAAC reaction) with Sauvage’s metal-template protocol. To underline our results, complementary model rotaxanes and catenanes have been prepared using the same strategy and their electrochemistry and photo-induced processes have been investigated. Insights into excited state interactions have been afforded from steady state and time resolved emission spectroscopy as well as transient absorption spectroscopy. It has been found that photo-excitation of the present rotaxanes triggers a cascade of multi-step energy and electron transfer events that ultimately leads to remarkably long-lived charge separated states featuring one-electron reduced  $\text{C}_{60}$  radical anion ( $\text{C}_{60}^{\cdot-}$ ) and either one-electron oxidized porphyrin ( $\text{ZnP}^{\cdot+}$ ) or one-electron oxidized ferrocene ( $\text{Fc}^{\cdot+}$ ) with lifetimes up to 61 microseconds. In addition, shorter-lived charge separated states involving one-electron oxidized copper complexes ( $[\text{Cu}(\text{phen})_2]^{2+}$  ( $\tau < 100$  ns)), one-electron oxidized zinc phthalocyanine ( $\text{ZnPc}^{\cdot+}$ ;  $\tau = 380$ –560 ns), or  $\text{ZnP}^{\cdot+}$  ( $\tau = 2.3$ –8.4  $\mu\text{s}$ ), and  $\text{C}_{60}^{\cdot-}$  have been identified as intermediates during the sequence. Detailed energy diagrams illustrate the sequence and rate constants of the photophysical events occurring with the mechanically-linked chromophores. This work pioneers the exploration of mechanically-linked systems as platforms to position three distinct chromophores, which are able to absorb light over a very wide range of the visible region, triggering a cascade of short-range energy and electron transfer processes to afford long-lived charge separated states.

Received 5th August 2015  
Accepted 17th September 2015

DOI: 10.1039/c5sc02895g  
[www.rsc.org/chemicalscience](http://www.rsc.org/chemicalscience)

## Introduction

In more than 25 years of fullerene research,  $\text{C}_{60}$  emerged as an excellent electron acceptor in electron transfer reactions, due to its unique properties. For instance, the rigid  $\text{C}_{60}$  cage can accept up to six electrons and has a very small reorganization energy in electron transfer reactions. Consequently,  $\text{C}_{60}$  has been utilized in photosynthetic reaction mimics, photovoltaics, and catalysis.<sup>1</sup> In order to guarantee efficient electron transfer, suitable electron donating moieties have to be chosen. In terms of

photosynthetic reaction mimics, they have to fulfill the redox requirements imposed by the fullerene as well as to have the ability to efficiently harvest light. Both of these specifications are met by tetrapyrrolic macrocycles, such as porphyrins and phthalocyanines.

An interesting alternative to spatially arrange the chromophores is provided by mechanically-interlocked systems, such as catenanes and rotaxanes, decorated with electron donors and electron acceptors.<sup>2–4</sup> These photo-active interlocked platforms have allowed the systematic investigation of the effects of molecular topology on the thermodynamic and kinetic parameters of the electron and energy transfer processes in artificial photosynthetic models. This effort is motivated by the need to better understand the intricate roles that the protein environment plays in the photo-induced processes in natural photosynthesis.<sup>5–10</sup>

For example, we have shown<sup>11</sup> that catenanes decorated with zinc porphyrin (ZnP) and  $\text{C}_{60}$  ultimately yield a charge separated state possessing  $\text{ZnP}^{\cdot+}$  and  $\text{C}_{60}^{\cdot-}$  radical ions with a lifetime

<sup>a</sup>Department of Chemistry and Pharmacy and Interdisciplinary Center for Molecular Materials, Friedrich-Alexander-Universität Erlangen-Nürnberg, D-91058 Erlangen, Germany. E-mail: [dirk.guldi@fau.de](mailto:dirk.guldi@fau.de)

<sup>b</sup>Department of Chemistry, New York University, New York, NY 10003, USA. E-mail: [david.schuster@nyu.edu](mailto:david.schuster@nyu.edu)

† Electronic supplementary information (ESI) available. See DOI: [10.1039/c5sc02895g](https://doi.org/10.1039/c5sc02895g)

‡ Present address: Institute of Chemistry, University of Campinas, PO Box 6154, Campinas, SP, 13084-861, Brazil.

roughly two times longer than the same charge separated state in the corresponding rotaxane.<sup>12</sup> This significant difference in lifetime reflects the distinct topology of the two interlocked systems. The catenane is conformationally rigid, while the rotaxane counterpart is not. Therefore, the former keeps the ZnP and C<sub>60</sub> moieties at longer and fixed distances, while the latter brings them closer to each other, a process that is driven by secondary interactions between the chromophores and allowed by the unclosed ring of the rotaxane.<sup>11-19</sup>

One of the well-established synthetic protocols to assemble rotaxanes and catenanes is Sauvage's Cu(i)-templated synthesis.<sup>20-24</sup> In this synthetic strategy, two 1,10-phenanthroline moieties (phen) become orthogonally arranged as a result of their tetrahedral coordination to the Cu(i) template ion, which creates the cross-over points needed for the formation of the mechanical bond. In the case of artificial photosynthetic models, the Cu(i) template synthesis ensures a further benefit, namely the presence of an additional photoactive unit, the [Cu(phen)<sub>2</sub>]<sup>+</sup> complex. It has been shown by us<sup>12,25</sup> and others<sup>26,27</sup> that the resulting [Cu(phen)<sub>2</sub>]<sup>+</sup> complex facilitates the electronic communication between appended electron donors and electron acceptors on rotaxanes and catenanes upon photoexcitation.

The present work reports that a minor variation of this strategy has allowed the incorporation of porphyrin, phthalocyanine, and ferrocene electron donors as stoppering groups of [Cu(phen)<sub>2</sub>]<sup>+</sup>-C<sub>60</sub> based rotaxanes to afford a new family of multi-chromophoric interlocked structures (Fig. 1) that are able

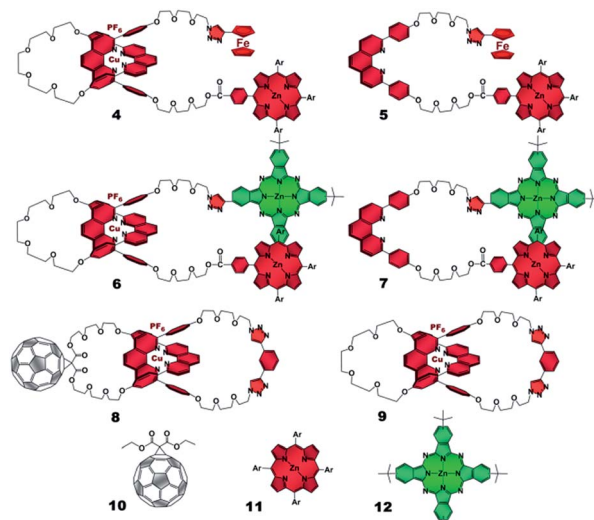


Fig. 2 Rotaxane and catenane models as well as reference compounds used to investigate the photophysical processes of the target rotaxanes.

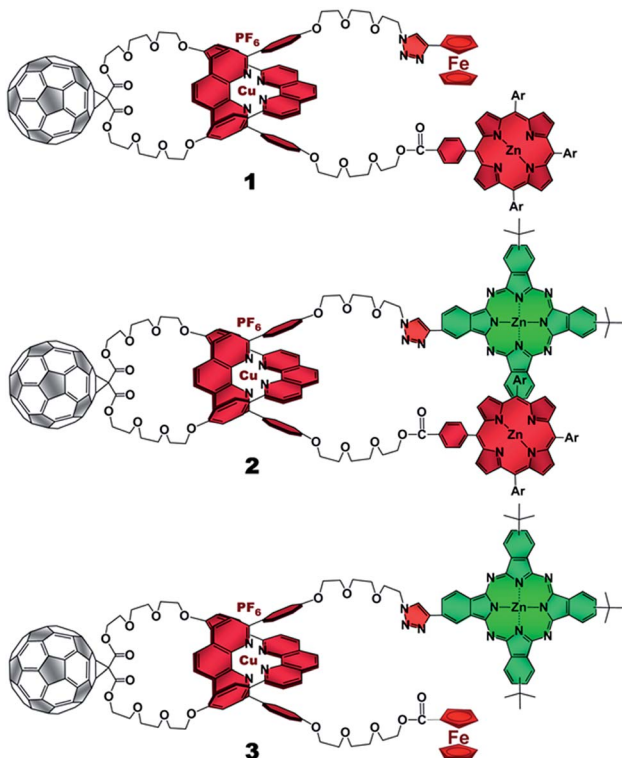


Fig. 1 [Cu(phen)<sub>2</sub>]<sup>+</sup>-C<sub>60</sub> based rotaxanes (1-3) stoppered by three different combinations of electron donors investigated in the present work. Ar = 3,5-di-*tert*-butylphenyl.

to undergo a cascade of energy and electron transfer reactions to yield charge separated states with remarkably long lifetimes. Furthermore, a complete set of model rotaxanes and catenanes lacking the electron donors, the C<sub>60</sub> or both, were prepared using our synthetic protocol and probed as reference systems (Fig. 2). A complete and systematic investigation of the new interlocked compounds by electrochemistry, UV-Vis absorption, steady state and time resolved emission spectroscopies as well as transient absorption spectroscopy in the femtosecond and nanosecond time regime has allowed us to gather the rates of the energy and electron transfer, charge shift, and charge recombination processes occurring upon photo-excitation of the three [Cu(phen)<sub>2</sub>]<sup>+</sup>-C<sub>60</sub> rotaxanes shown in Fig. 1 to elucidate their deactivation processes.

## Results and discussion

### 1. Synthesis

The synthetic strategy used to prepare rotaxanes 1-3 is depicted in Scheme S1 (see ESI†). Briefly, one of the hydroxyl groups of compound 13<sup>11</sup> is tosylated under classical conditions to yield 14, which undergoes a nucleophilic substitution with sodium azide to afford 15. The remaining hydroxyl group in 15 is esterified using 1-ethyl-3-(3-dimethyl-aminopropyl)carbodiimide (EDC) as coupling agent and dimethylaminopyridine (DMAP) as base following the conditions reported in the experimental section (see ESI†) with either porphyrin 16<sup>28</sup> or commercially available ferrocenecarboxylic acid 21 to produce the phen derivatives 17 and 22, respectively. Threading of 17 or 22 through the C<sub>60</sub>-based phen-macrocycle 18 using [Cu(CH<sub>3</sub>CN)<sub>4</sub>]PF<sub>6</sub> as the Cu(i) source in a mixture of dichloromethane/acetonitrile (7 : 3, v/v) at room temperature and under nitrogen atmosphere quantitatively yielded pseudo-rotaxanes 19 and 23, respectively, as revealed by TLC. Finally, pseudo-rotaxanes 19 or 23 and commercially available alkynyl ferrocene or



phthalocyanine **20**<sup>29</sup> were submitted to our “click” protocol<sup>11,17,30</sup> to afford the target rotaxanes **1**, **2**, and **3**. Rotaxane and catenane model compounds were prepared following the same strategy from the appropriate building blocks.

## 2. Ground state interactions – absorption spectra and electrochemistry

The absorption spectra of rotaxanes **1–3** feature the typical absorption characteristics of the various building blocks (Fig. 3). In particular, rotaxane **1** exhibits broad absorption between 300 and 380 nm, corresponding to  $C_{60}$  and  $[Cu(phen)_2]^+$ . ZnP with its Soret and Q-bands reveals absorptions at 432, 561, and 602 nm. Compared to ZnTPP **11**, the ZnP absorption bands exhibit a red shift of around 3 nm. Ferrocene is spectroscopically invisible in the 300 to 800 nm range. Rotaxane **2** features additional absorption maxima corresponding to ZnPc, namely Soret and Q bands at 340, 616, and 685 nm. Here, the ZnP absorption bands are 2 nm red shifted compared to **1** or masked by the ZnPc absorption. Similarly, the absorption of  $C_{60}$  and  $[Cu(phen)_2]^+$  is covered by that of ZnPc. The absorption spectrum of rotaxane **3** is dominated by the features corresponding to ZnPc, that is, maxima at 345, 613 and 679 nm, which are ~6 nm red shifted compared to ZnPc reference compound **12**. Increased extinction coefficients in the Soret band region stem from  $C_{60}$  and  $[Cu(phen)_2]^+$  absorptions.

Turning to electrochemistry (see Table S1†) the redox chemistry of rotaxane **1** is best described as the superposition of catenane **8**, ZnTPP **11**, and ferrocene. In particular, two one-electron reductions are seen within the electrochemical window of the solvent (dichloro-methane) at –1.09 and –1.45 V (all redox potentials are relative to  $Fe/Fe^+$ ). Both are assigned to  $C_{60}$  centered reductions. Three oxidations are observed. As in rotaxane **4**, the first oxidation at +0.04 V is assigned to Fc, while the second, more intense oxidation at +0.24 V corresponds to a  $[Cu(phen)_2]^+$ -centered process as well as to the first ZnP oxidation. Likewise, the third oxidation at +0.88 V correlates with the second ZnP oxidation.

Rotaxane **2** exhibits all the redox features seen for ZnTPP **11**,  $Zn^tBu_4Pc$  **12**, and catenane **8**. To be more precise, two

reductions at –1.13 and –1.54 V correspond to the reduction of  $C_{60}$ , while the oxidation of  $[Cu(phen)_2]^+$  is observed at +0.13 V. As seen for **6** and **7**, the first ZnP and ZnPc oxidations cannot be clearly distinguished. A broader and more intense feature at +0.18 V is attributed to both. The second ZnP oxidation is observed at +0.83 V.

Finally, rotaxane **3** features two oxidations as well as two reductions within the electrochemical window. Here, the ferrocene oxidation is slightly shifted to less negative potentials, namely –0.05 V, possibly due to interactions with the other chromophores, while the second oxidation with about twice the intensity, is assigned to the one-electron oxidations of ZnPc and  $[Cu(phen)_2]^+$ . The reductive scan indicates two reductions of  $C_{60}$  at –1.10 and –1.55 V. The redox potentials of compounds **1–12** are summarized in Table S1 in the ESI.†

## 3. Excited state interactions - fluorescence

Table S2† lists the fluorescence properties of the investigated rotaxanes as well as the corresponding reference compounds. The strongest fluorescent chromophore is ZnPc reference compound **12**, with a fluorescence quantum yield of 0.3.<sup>31,32</sup> Its fluorescence spectrum shows a maximum at 779 nm in THF – Fig. S4† – and at 790 nm in PhCN – Fig. S5.† ZnTPP **11**, with maxima at 602 and 655 nm in THF and 609 and 660 nm in PhCN, exhibits much weaker fluorescence with a quantum yield of 0.04.

In contrast, the ZnP fluorescence in rotaxanes **1** and **4** is significantly quenched. Upon excitation at 420 nm, which coincides with the Soret band absorption maximum, a relatively weak ZnP fluorescence of 0.02 (Table S2†) is observed for **1** and **4**, while in **5** the ZnP fluorescence is not quenched at all, which suggests energy and/or electron transfer from ZnP to  $[Cu(phen)_2]^+$  and  $C_{60}$  occurs in **1** and **4**.

In rotaxane **2**, as well as in reference compounds **6** and **7**, the ZnPc fluorescence is quenched compared to **12** and the maximum emission is shifted to longer wavelengths. They show ZnPc fluorescence quantum yields between 0.07 and 0.13 in THF (Table S2†) and between 0.09 and 0.24 in PhCN. The ZnP emission in rotaxanes **2** and **6** as well as in reference compound **7** is even more strongly quenched. Upon excitation into the porphyrin's Soret band at 420 nm only weak porphyrin fluorescence ranging from 0.004 to 0.008 (Table S2†) is observed, which is partly overlaid by a strong fluorescence maximizing at ~690 nm with a shoulder at 760 nm (Fig. 4, top).

Glancing at the excitation spectrum of **2** (Fig. 4 bottom) it is clear that this fluorescence originates from ZnPc, since the excitation spectrum corresponding to the 760 nm emission combines features of ZnP as well as of ZnPc. In contrast, the excitation spectrum of the 600 nm feature clearly proves that this fluorescence originates exclusively from ZnP. Thus, we postulate that an energy transfer from ZnP (2.06 eV) to the energetically lower lying ZnPc (1.8 eV) takes place. The quantum yield for this energy transfer was found to be 0.04 for rotaxane **2** in THF.

Rotaxane **3** exhibits 50% quenched ZnPc fluorescence – Table S2.† This quenching gives rise to the conclusion that

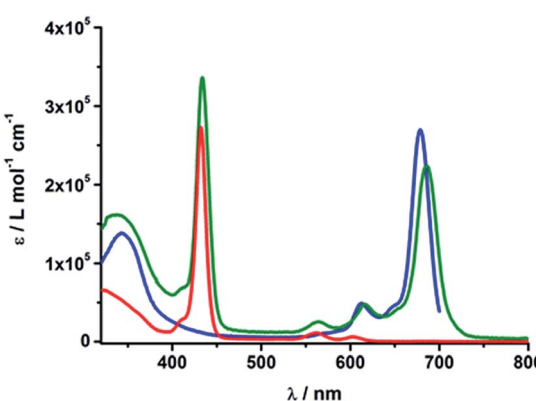


Fig. 3 UV/Vis absorption spectra of  $Fc-ZnP-[Cu(phen)_2]^+-C_{60}$  **1** (red),  $ZnP-ZnPc-[Cu(phen)_2]^+-C_{60}$  **2** (olive) and  $Fc-ZnPc-[Cu(phen)_2]^+-C_{60}$  **3** (blue) in PhCN.



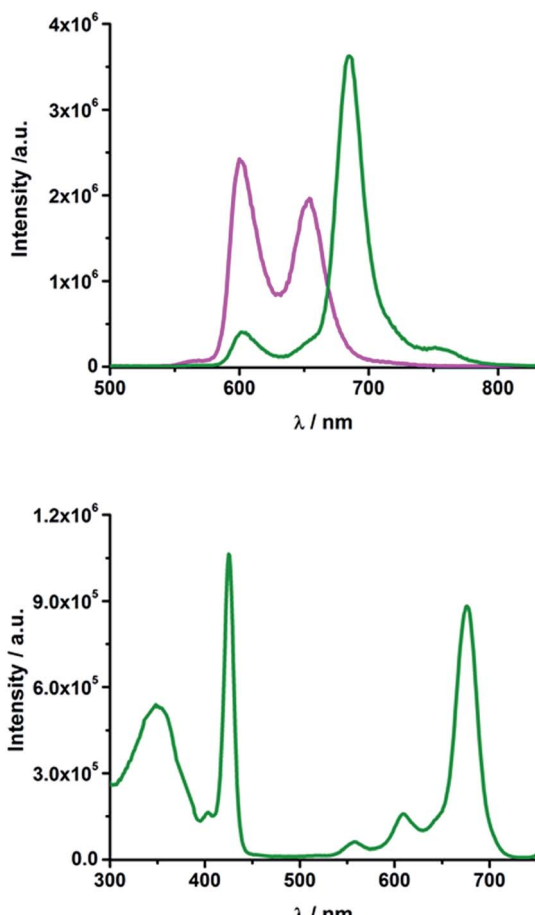


Fig. 4 Top: Emission spectrum of rotaxane 2 (olive) and ZnTPP 11 (magenta) in THF upon excitation at 420 nm ( $OD = 0.084$ ); bottom: excitation spectrum of rotaxane 2 in THF for emission at 760 nm.

energy and/or electron transfer from ZnPc to  $[\text{Cu}(\text{phen})_2]^+$  and to  $\text{C}_{60}$  takes place in these rotaxanes.

#### 4. Excited state interactions – transient absorption spectroscopy

To obtain information about the formation and decay processes of the excited states upon photoexcitation, transient absorption spectroscopy was carried out with rotaxanes 1–3 as well as reference compounds 4–12 (see ESI†) in THF using fs (387, 420 and 660 nm) as well as ns (355, 425 and 670 nm) laser excitation. Notably, we assume that the electron transfer processes are driven by through-space rather than through-bond interactions.

The transient absorption spectrum of rotaxane 1 – Fig. 5 – is dominated by features that can be assigned to the singlet and triplet excited states  $\text{ZnP}^+$ . In the near infrared region features corresponding to  $^3\text{MLCT}^*$  and  $^1\text{*C}_{60}$  are discernible. As time progresses, all of the aforementioned characteristics are replaced by a weak maximum at 1020 nm, which correlates with the fingerprint absorption of the one electron reduced form of  $\text{C}_{60}$ .<sup>11,12,16,34</sup> This is stable on the 7.5 ns timescale of our experimental setup. The signature of the one electron oxidized form of either  $[\text{Cu}(\text{phen})_2]^+$ , ZnP, or Fc – as a complement to the one electron reduced form of  $\text{C}_{60}$  – are not discernible due to

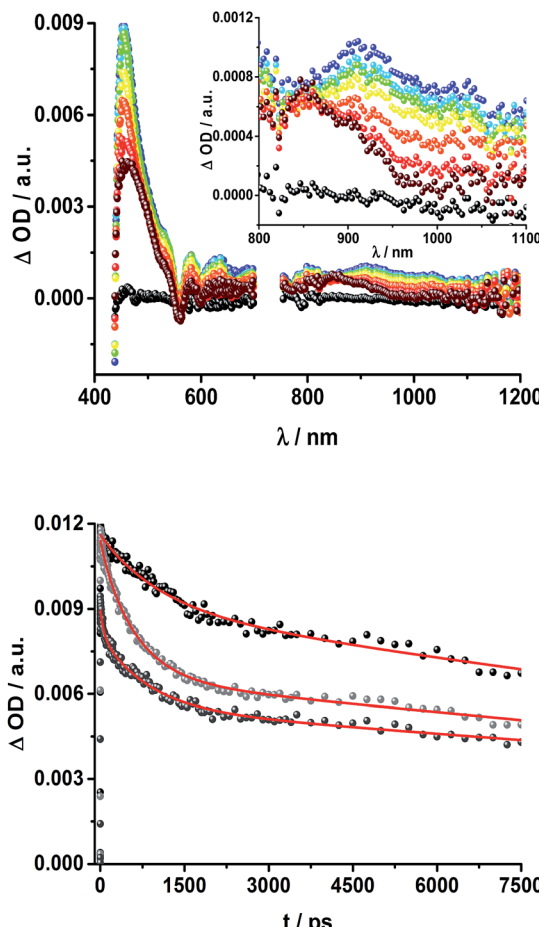


Fig. 5 Top: Transient absorption spectrum (visible and near-infrared) registered upon femtosecond flash photolysis (420 nm, 150 nJ) of Fc-ZnP- $[\text{Cu}(\text{phen})_2]^+$ - $\text{C}_{60}$  rotaxane 1 in THF with time delays between 0 (black) and 7.5 ns (wine) at room temperature. Inset: zoom into the near infrared region. Bottom: Time absorption profiles of 1 (dark grey), 4 (grey), and 5 (black) at 455 nm upon excitation with a 420 nm laser pulse, monitoring the decay of the ZnP singlet excited state.

dominating ZnP singlet and triplet absorption features. The fact that the broad near-infrared transient is formed independently of the excitation wavelength leads us to conclude that energy transfer from ZnP to  $[\text{Cu}(\text{phen})_2]^+$  takes place. When comparing rotaxanes 1 and 4, the ZnP fluorescence is quenched by 50% relative to ZnTPP 11 in both cases. Thus, the lack of energy transfer to  $\text{C}_{60}$  is hypothesized (Fig. 5).

**4.1 Rotaxane 1.** Complementary transient absorption measurements on the ns timescale under aerobic conditions as well as in argon-saturated THF shed light upon the excited state interactions in rotaxane 1. Upon excitation at 425 nm, the differential absorption spectra are dominated by ZnP-centered features, namely the ZnP triplet excited state with a broad absorption throughout the visible region and maxima at 460 and 840 nm (Fig. 6). In the absence of oxygen, a ZnP triplet excited state lifetime of  $142 \pm 12 \mu\text{s}$  was determined for rotaxane 1 in THF (Fig. 7). Notable is the fact that the triplet excited state of  $\text{C}_{60}$  gives rise to a transient maximum at 740 nm, whose formation is masked by the dominating ZnP triplet excited state

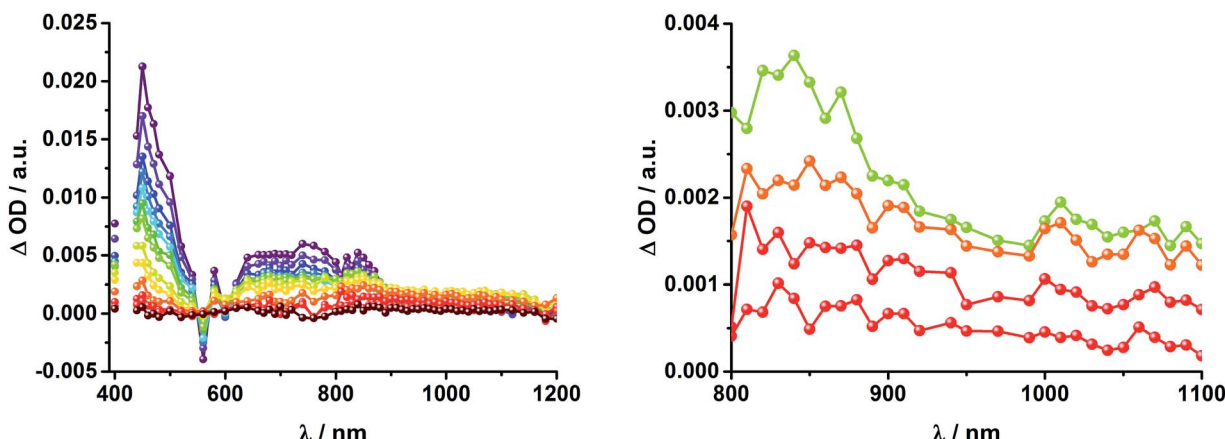


Fig. 6 Left: Differential absorption spectra (visible and near infrared) registered upon nanosecond flash photolysis (425 nm, 5 mJ) of  $\text{Fc-ZnP}-[\text{Cu}(\text{phen})_2]^+-\text{C}_{60}$  rotaxane **1** under aerobic conditions in THF with time delays between 200 ns (purple) and 15  $\mu\text{s}$  (wine) at room temperature. Right: Differential absorption spectra (near infrared) registered upon nanosecond flash photolysis (425 nm, 5 mJ) of  $\text{Fc-ZnP}-[\text{Cu}(\text{phen})_2]^+-\text{C}_{60}$  rotaxane **1** under aerobic conditions in THF with time delays between 1 (green) and 5  $\mu\text{s}$  (red) at room temperature.

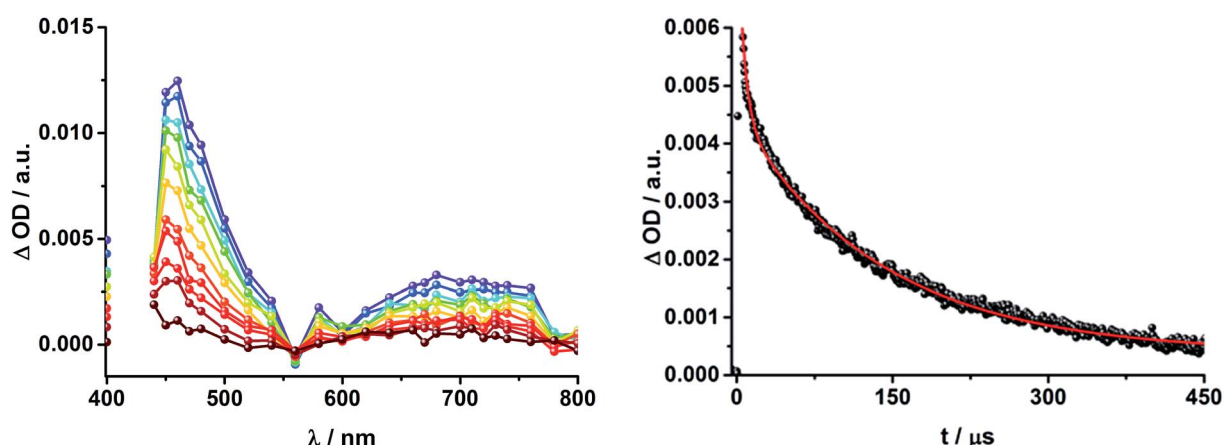


Fig. 7 Left: Differential absorption spectra (visible) registered upon nanosecond flash photolysis (425 nm, 5 mJ) of  $\text{Fc-ZnP}-[\text{Cu}(\text{phen})_2]^+-\text{C}_{60}$  rotaxane **1** under argon atmosphere in THF with time delays between 8  $\mu\text{s}$  (purple) and 400  $\mu\text{s}$  (wine) at room temperature. Right: Time absorption profile of the spectra on the left at 460 nm, monitoring the decay of the ZnP triplet excited state.

features.<sup>11,12</sup> A closer look at the differential absorption changes reveals additional peaks discernible at 680 and 1010 nm (Fig. 6). In line with previous reports, the latter is assigned to the one electron reduced form of  $\text{C}_{60}$ , while the former correlates with the one electron oxidized form of ZnP.<sup>11,14,15,18,33,35</sup> From the corresponding extinction coefficients, that is,  $0.82 \times 10^4 \text{ M}^{-1} \text{ cm}^{-1}$  for the ZnP triplet excited state at 840 nm<sup>36</sup> and  $1.5 \times 10^4 \text{ M}^{-1} \text{ cm}^{-1}$  for the one electron reduced form of  $\text{C}_{60}$ ,<sup>37</sup> we conclude that the major product is the former. However, exact values for the yields of charge separation could not be determined. Accordingly, upon ns-excitation of rotaxane **1** a long-lived  $\text{ZnP}^+/\text{C}_{60}^-$  charge separated state is formed in addition to the ZnP triplet excited state. Evidence for the transient formation of one electron oxidized ferrocene and/or  $[\text{Cu}(\text{phen})_2]^+$  is hampered by their very low extinction coefficients.<sup>38-43</sup> Interactions by energy transfer are unlikely to happen for energetic reasons but cannot be ruled out with certainty.

To dissect the different contributions to the transient absorption spectra on rotaxane **1**, that is, the charge separated states, the ZnP triplet excited state, and the  $\text{C}_{60}$  triplet excited state, the decay kinetics of the one electron oxidized form of ZnP at 680 nm and the one electron reduced form of  $\text{C}_{60}$  at 1010 nm were examined in the presence or absence of oxygen. It is well known that oxygen impacts the triplet excited state lifetime of ZnP (Table S3†).<sup>44,45</sup> We find that the transient at 680 nm decays biexponentially (Fig. S10,† left) with one lifetime that depends strongly on the  $\text{O}_2$  concentration and another one that is nearly constant; 112  $\mu\text{s}$  is the lifetime in the absence of  $\text{O}_2$  and 110 ns under  $\text{O}_2$  saturated conditions (Table S3†), from which a bimolecular quenching rate constant of  $1.0 \times 10^9 \text{ M}^{-1} \text{ s}^{-1}$  is derived. The other component has a nearly constant lifetime of  $2.3 \pm 0.3 \mu\text{s}$ . The  $\text{O}_2$ -dependent lifetime must relate to the ZnP triplet excited state, whereas the component that shows only a weak  $\text{O}_2$  dependence is assigned to the charge separated state

involving  $\text{ZnP}^{+}$ . Note that the extinction coefficient of the one electron oxidized form of  $\text{Fc}$  is lower than that of  $\text{ZnP}$  with a value of  $500 \text{ M}^{-1} \text{ cm}^{-1}$ .<sup>15</sup> In light of the aforementioned, we analyzed the decay of  $\text{C}_{60}^{\cdot-}$  – Fig. S10† – at 1010 nm. From tri-exponential fittings a short lifetime of  $55 \pm 8 \text{ ns}$  as well as an intermediate and a long lifetime of  $2.3 \pm 0.4$  and  $61 \pm 16 \mu\text{s}$  were derived. Only the intermediate and long lifetimes exhibit dependence on the concentration of  $\text{O}_2$ , yielding bimolecular rate constants of  $1.0 \times 10^7$  and  $1.7 \times 10^5 \text{ M}^{-1} \text{ s}^{-1}$ , respectively. Considering that the short lifetime is comparable to that found for **8**<sup>1,12,18,33</sup> it is, in turn, assigned to  $\text{Fc-ZnP-[Cu(phen)}_2^{\cdot+}-\text{C}_{60}^{\cdot-}$ . The intermediate lifetime of the 1010 nm decay matches the 680 nm decay, which suggests that it is the  $\text{Fc-ZnP}^{+}-[\text{Cu(phen)}_2^{\cdot+}-\text{C}_{60}^{\cdot-}$  charge separated state. Finally, the long lifetime is assigned to the  $\text{Fc}^{+}-\text{ZnP-[Cu(phen)}_2^{\cdot+}-\text{C}_{60}^{\cdot-}$  long distance charge separated state, since it possesses the lowest energy (1.13 eV).

Fig. 8 schematically summarizes the processes which take place upon 425 nm excitation of rotaxane **1** with the corresponding energy levels calculated from spectroscopic and electrochemical data. Excitation of rotaxane **1** into the  $\text{ZnP}$  Soret band at 425 nm generates the  $\text{ZnP}$  singlet excited state with an energy level of 2.06 eV relative to the ground state. From these states, different deactivation pathways emerge. Firstly, a deactivation to the ground state *via* fluorescence occurs with a quantum yield of 2%. Secondly, intersystem crossing (ISC) yields the energetically lower-lying  $\text{ZnP}$  centered triplet excited state (1.50 eV), which subsequently decays to the ground state. In competition, energy transfer from the  $\text{ZnP}$  singlet excited state to  $[\text{Cu(phen)}_2]^{\cdot+}$  takes place. The energy transduction to  $[\text{Cu(phen)}_2]^{\cdot+}$  is followed by a rapid and unresolvable ISC to  ${}^3\text{MLCT}^*$ . From the latter, electron transfer generates  $\text{C}_{60}^{\cdot-}$  and  $[\text{Cu(phen)}_2]^{2+}$  with an energy level at 1.31 eV above the ground state. Experimental confirmation for this electron transfer hypothesis comes from comparison between the ns transient absorption data for **1** with those obtained for catenane **8**. The lifetime of  $\text{C}_{60}^{\cdot-}$  of 55 ns ( $k_{\text{CR}} = 1.8 \times 10^7 \text{ s}^{-1}$ ) in **1** resembles

that found for catenane **8** (100 ns).<sup>11,12,16,33</sup> Despite the fact that  $[\text{Cu(phen)}_2]^{2+}$  cannot be identified in the differential absorption spectra, due to its low extinction coefficient, we are confident about the formation and existence of the  $\text{Fc-ZnP-[Cu(phen)}_2^{\cdot+}-\text{C}_{60}^{\cdot-}$  charge separated state. From this intermediate state, a charge shift process occurs from  $[\text{Cu(phen)}_2]^{2+}$  to ferrocene and/or to  $\text{ZnP}$ . On longer time scales, two additional lifetimes were derived for the one electron reduced  $\text{C}_{60}$ , one of which matches the lifetime of  $2.3 \mu\text{s}$  ( $k_{\text{CR}} = 4.3 \times 10^5 \text{ s}^{-1}$ ) found for the one electron oxidized  $\text{ZnP}$  at 680 nm. Accordingly, this lifetime is assigned to the  $\text{Fc-ZnP}^{+}-[\text{Cu(phen)}_2]^{\cdot+}-\text{C}_{60}^{\cdot-}$  charge separated state, which is apparently isoenergetic with the  $\text{Fc-ZnP-[Cu(phen)}_2^{\cdot+}-\text{C}_{60}^{\cdot-}$  one, which favors interaction between these two states. The lifetime of  $61 \mu\text{s}$  ( $k_{\text{CR}} = 1.6 \times 10^4 \text{ s}^{-1}$ ) is attributed to the  $\text{Fc}^{+}-\text{ZnP-[Cu(phen)}_2^{\cdot+}-\text{C}_{60}^{\cdot-}$  long distance charge separated state. This state is expected to be the thermodynamically most stable state at 1.13 eV relative to the ground state (Fig. 8). This stable state can be generated by two thermodynamically possible charge shift scenarios, that is, one evolving from  $\text{Fc-ZnP-[Cu(phen)}_2^{\cdot+}-\text{C}_{60}^{\cdot-}$  and the other from  $\text{Fc-ZnP}^{+}-[\text{Cu(phen)}_2]^{\cdot+}-\text{C}_{60}^{\cdot-}$ . Considering the slow charge recombination in  $\text{Fc}^{+}-\text{ZnP-[Cu(phen)}_2^{\cdot+}-\text{C}_{60}^{\cdot-}$ , with a rate constant of  $k_{\text{CR}} = 1.6 \times 10^4 \text{ s}^{-1}$ , it is clear that charge recombination is located in the inverted region of the Marcus parabola.<sup>46,47</sup>

**4.2 Rotaxane 2.** Excitation of rotaxane **2** at 660 nm yields the  $\text{ZnPc}$  singlet excited state identified by the 825 nm transient absorption.<sup>31,43</sup> The latter deactivates *via* ISC. The  $\text{ZnPc}$  triplet excited state with its 490 nm marker is stable on the time scale of the experiment. Ground state bleaching is observed at 610 and 680 nm. Additionally, a new peak in the near infrared region at 1010 nm emerges, which is the fingerprint of  $\text{C}_{60}^{\cdot-}$ .<sup>11,12,44</sup> From this, we conclude that electron transfer takes place in rotaxane **2** in competition with ISC. Excitation into the  $\text{ZnP}$  Soret band of **2** at 420 nm results in population of the  $\text{ZnP}$  singlet excited state which decays within 40 ps to give the  $\text{ZnP}$  triplet excited state as well as the energetically lower lying  $\text{ZnPc}$  singlet excited state, as found for **6** and **7** (ESI†). In this case, no clear signs for any transduction of excited state energy were found.

Upon excitation of rotaxane **2** at 387 nm, not only the  $\text{ZnP}$  and  $\text{ZnPc}$  transient features are observed in the differential absorption spectra, as seen upon 660 and 420 nm excitation, but also those of  $\text{C}_{60}$  and  $[\text{Cu(phen)}_2]^{\cdot+}$  (Fig. 9). In the visible region of the spectrum, the  $\text{C}_{60}$  singlet excited state marker at 510 nm and  ${}^3\text{MLCT}^*$  marker at 600 nm are masked by the more intense  $\text{ZnP}$  and  $\text{ZnPc}$  transient absorptions. In the near-infrared region, a rather broad transient absorption is observed that corresponds to the triplet  $\text{MLCT}$  state. Additionally, two maxima are identified at 850 and 1020 nm in PhCN or 840 and 1020 nm in THF. The 1020 nm transient, the well-known fingerprint of  $\text{C}_{60}^{\cdot-}$ , is stable over the 7.5 ns time scale of our experiment.<sup>48,49</sup> The 840–850 nm transient corresponds to the  $\text{ZnPc}$  singlet excited state with a lifetime of 2.2 ns in PhCN and 1.6 ns in THF. Notably, mono-exponential fitting is not sufficient to describe the underlying transient decay. The 850 nm transient, which is stable over the 7.5 ns time scale, can be

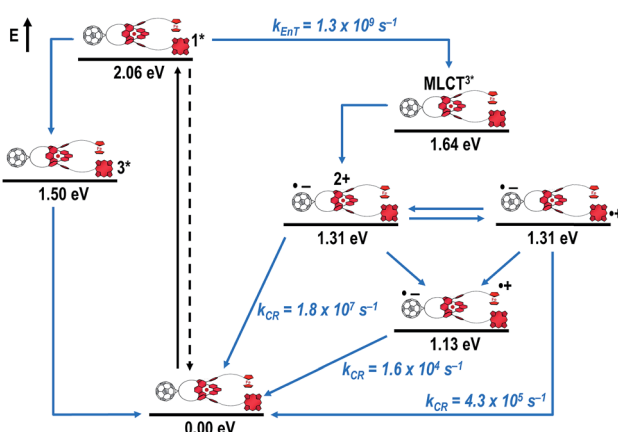


Fig. 8 Schematic energy level diagrams, proposed decay pathways, and rate constants for  $\text{Fc-ZnP-[Cu(phen)}_2^{\cdot+}-\text{C}_{60}^{\cdot-}$  rotaxane **1** upon excitation at 425 nm.  $k_{\text{EnT}}$  = energy transfer rate;  $k_{\text{CR}}$  = charge recombination rate constant.



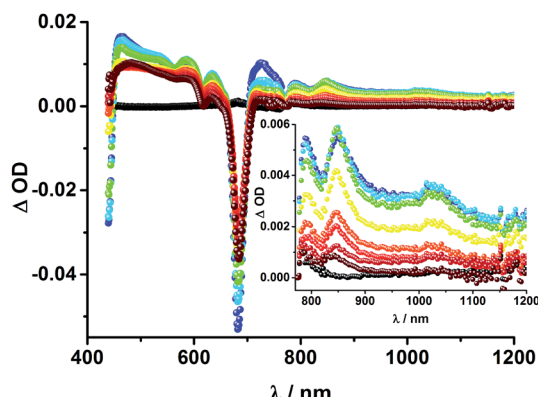


Fig. 9 Transient absorption spectrum (visible and near-infrared) registered upon femtosecond flash photolysis (387 nm, 200 nJ) of ZnP-ZnPc-Cu(phen)<sub>2</sub>-C<sub>60</sub> rotaxane 2 in PhCN with time delays between 0 (black) and 7.5 ns (wine) at room temperature. Inset: enhanced spectra in near infrared region.

assigned to the one electron oxidized ZnPc.<sup>50</sup> Thus, we conclude that electron transfer from ZnPc to C<sub>60</sub> takes place. The possibility that ZnP is also involved in an electron transfer process cannot be ruled out, since its transient features coincide with the ZnPc ground state bleaching. However, based on thermodynamics we conclude this pathway is very unlikely.

In complementary ns-transient absorption experiments, rotaxane 2 was excited into the ZnP Soret band at 425 nm and into the ZnPc Q-band at 670 nm. Upon ZnPc excitation, the visible region of the differential absorption spectra is dominated by the broad ZnPc triplet excited state signature at 480 nm (Fig. 10, left). The latter is oxygen sensitive, with lifetimes of  $\sim$ 300 ns in the presence of oxygen and  $\sim$ 14  $\mu$ s in the absence of oxygen. Absorption signatures corresponding to C<sub>60</sub> triplet excited state and/or <sup>3</sup>MLCT\* were not observed due to the intense ZnPc ground state bleaching between 650 and 750 nm.

In the near-infrared region, two maxima are discernible at 850 and 1010 nm. The former is assigned to the one-electron oxidized ZnPc, which decays with a lifetime of  $\sim$ 520  $\pm$  100 ns, while the latter is the one-electron reduced C<sub>60</sub> and exhibits two decay lifetimes, 64  $\pm$  26 ns and 570  $\pm$  110 ns. The shorter lifetime matches those found for reference compound 8<sup>11,12,16,33</sup> and the close charge separated states in rotaxane 1. Thus, it is assigned to the [Cu(phen)<sub>2</sub>]<sup>+</sup> centered charge separated state ZnP-ZnPc-[Cu(phen)<sub>2</sub>]<sup>2+</sup>-C<sub>60</sub><sup>.-</sup>. The longer lifetime is in agreement with the ZnP-ZnPc<sup>+-</sup>-[Cu(phen)<sub>2</sub>]<sup>+</sup>-C<sub>60</sub><sup>.-</sup> long distance charge separated state. No indication of a charge shift to form ZnP<sup>+-</sup>-ZnPc-[Cu(phen)<sub>2</sub>]<sup>+</sup>-C<sub>60</sub><sup>.-</sup> was seen upon 670 nm excitation.

When exciting into the ZnP Soret band at 425 nm, the transient absorption spectra are slightly different (Fig. 10, right). Here, the dominant features belong to those of ZnP with maxima at 480 and 840 nm. The biexponential decay of the 480 nm transients, gives lifetimes corresponding to the triplet excited state of ZnP (140  $\mu$ s under Ar) as well as that of ZnPc (14  $\mu$ s under Ar). Thus, it is reasonable to assume that upon excitation of ZnP two deactivation pathways occur; ISC to the triplet manifold and energy transfer to ZnPc followed by ISC. This observation is also in agreement with the fs transient absorption data. In addition to the strongly oxygen dependent ZnPc triplet excited state lifetime, the decay at 840 nm yields a second component with a lifetime of 560  $\pm$  100 ns. This lifetime correlates with that seen for ZnPc<sup>+</sup>, as seen upon 670 nm excitation. Furthermore, the decay of C<sub>60</sub><sup>.-</sup> at  $\sim$ 1010 nm can be fit with three lifetimes, 63  $\pm$  16 ns, 590  $\pm$  150 ns, and 8.4  $\pm$  1.0  $\mu$ s (Fig. 11). Again, the shortest lifetime is assigned to ZnP-ZnPc-[Cu(phen)<sub>2</sub>]<sup>2+</sup>-C<sub>60</sub><sup>.-</sup>. In contrast to the 670 nm excitation, in this case two different charge shifts seem to occur. Firstly, the ZnPc centered charge separated state ZnP-ZnPc<sup>+-</sup>-[Cu(phen)<sub>2</sub>]<sup>+</sup>-C<sub>60</sub><sup>.-</sup> with a lifetime of 560  $\pm$  120 ns (from 840 and 1010 nm decays) is formed. Secondly, the longer lived ZnP

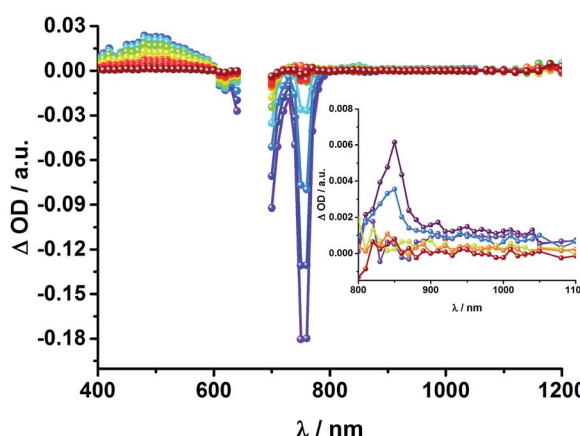
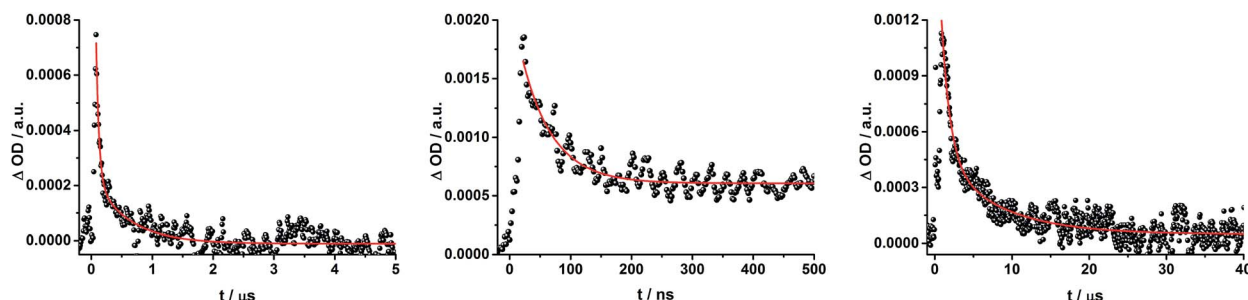


Fig. 10 Left: Differential absorption spectra (visible and near infrared) registered upon nanosecond flash photolysis (670 nm, 5 mJ) of ZnP-ZnPc-[Cu(phen)<sub>2</sub>]<sup>+-</sup>-C<sub>60</sub> rotaxane 2 under aerobic conditions in THF with time delays between 90 ns (blue) and 1.0  $\mu$ s (wine) at room temperature. Inset: zoom into the near infrared region with time delays between 65 ns (purple) and 1.0  $\mu$ s (wine). Right: Differential absorption spectra (visible and near infrared) registered upon nanosecond flash photolysis (425 nm, 5 mJ) of ZnP-ZnPc-[Cu(phen)<sub>2</sub>]<sup>+-</sup>-C<sub>60</sub> rotaxane 2 under aerobic conditions in THF with time delays between 120 ns (blue) and 4.0  $\mu$ s (wine) at room temperature. Inset: expanded spectra in the near infrared region with time delays between 23 ns (purple) and 400 ns (green).





**Fig. 11** Time absorption profiles at 1010 nm of ZnP-ZnPc-[Cu(phen)<sub>2</sub>]<sup>+</sup>-C<sub>60</sub> rotaxane 2 in THF at room temperature under aerobic conditions upon excitation at 670 nm (left) and 425 nm (center and right), monitoring the charge recombination.

centered charge separated state  $\text{ZnP}^{+}-\text{ZnPc}-[\text{Cu}(\text{phen})_2]^{+}-\text{C}_60^{-}$  with a lifetime of  $8.4 \mu\text{s}$  is generated. The corresponding cation again cannot be identified, since it coincides with the ZnPc ground state bleaching in the  $680 \text{ nm}$  region. Overall, these results are in agreement with the transient lifetimes found for rotaxane **1**. A schematic energy level diagram of the photoinduced processes in rotaxane **2** is shown in Fig. 12, including energy levels calculated from electrochemical and spectroscopic data. Two different excitation routes are feasible, which result in slightly different deactivation processes. When exciting ZnPc at  $670 \text{ nm}$ , its singlet excited state is immediately formed, with an energy level of  $1.81 \text{ eV}$  relative to the ground state. Deactivation *via* fluorescence (12%) as well as *via* ISC takes place. In parallel, energy transfer from the ZnPc singlet excited state to  $[\text{Cu}(\text{phen})_2]^{+}$  occurs, which is verified by  $\sim 80\%$  quenching of the ZnPc fluorescence (Table S2†). Next, the  ${}^1\text{MLCT}$  undergoes rapid ISC to give  ${}^3\text{MLCT}^*$  ( $1.64 \text{ eV}$ ). By analogy to **1**, the  ${}^3\text{MLCT}^*$  decays through electron transfer to yield the charge separated state  $\text{ZnP}-\text{ZnPc}-[\text{Cu}(\text{phen})_2]^{2+}-\text{C}_60^{-}$ . The rate constant for the charge recombination of  $\text{ZnP}-\text{ZnPc}-[\text{Cu}(\text{phen})_2]^{2+}-\text{C}_60^{-}$  is  $1.6 \times 10^7 \text{ s}^{-1}$  ( $63 \text{ ns}$ ), in the same range

as that observed for **8**<sup>11,12,18,33</sup> and **1**. A charge shift from the oxidized  $[\text{Cu}(\text{phen})_2]^{2+}$  to ZnPc yields the charge separated state ZnP-ZnPc $^{+}$ - $[\text{Cu}(\text{phen})_2]^{2+}$ - $\text{C}_{60}^{-}$ , whose formation is corroborated by the observation of the same lifetimes (560 ns,  $k_{\text{CR}} = 1.8 \times 10^6 \text{ s}^{-1}$ ) for the one electron oxidized ZnPc and the one electron reduced  $\text{C}_{60}^{-}$ . No proof for the formation of the ZnP centered charge separated state was found upon 670 nm excitation. However, when exciting rotaxane **2** at 425 nm, the ZnP singlet excited state (2.06 eV) is formed and additional decay pathways emerge. On one hand, the ZnP triplet excited state ( $\sim 1.5$  eV) is generated *via* ISC, which decays back to the ground state. On the other hand, energy transfer to the energetically lower lying  ${}^1\text{ZnPc}$  (1.81 eV) takes place, which has been observed by fluorescence as well as excitation spectra (Fig. 4 and Table S2†). From this point on, the same processes occurring upon excitation at 670 nm take place. However, when taking a closer look at  $\text{C}_{60}^{-}$  decay at 1010 nm, a third much longer lifetime of 8.4  $\mu\text{s}$  ( $k_{\text{CR}} = 1.2 \times 10^5 \text{ s}^{-1}$ ) was identified. Consequently, we conclude that upon excitation of rotaxane **2** at 425 nm, a second charge shift from ZnP-ZnPc $^{+}$ - $[\text{Cu}(\text{phen})_2]^{2+}$ - $\text{C}_{60}^{-}$  takes place to form the ZnP centered long distance charge

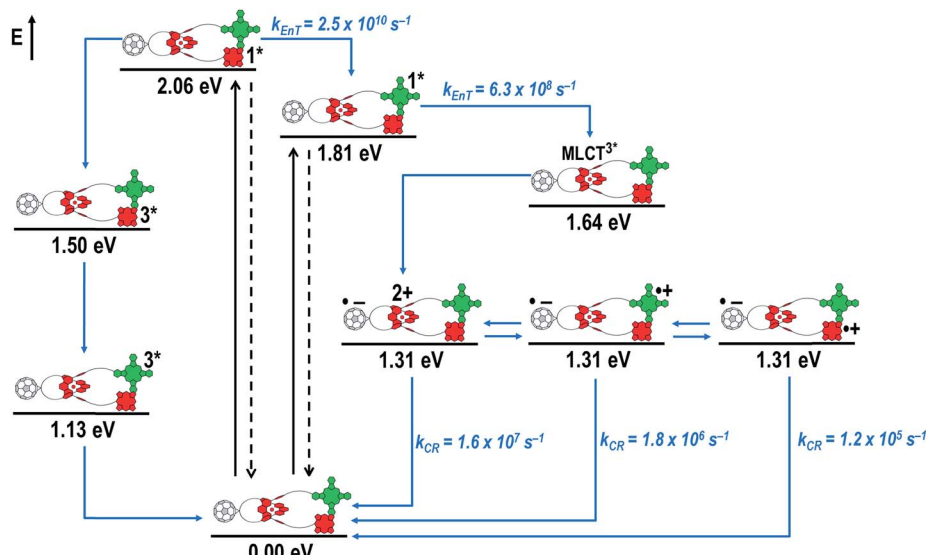


**Fig. 12** Schematic energy level diagrams, proposed decay pathways, and rate constants for ZnP–ZnPc–[Cu(phen)]<sup>+</sup>–C<sub>60</sub> rotaxane **2** upon excitation at 425 nm and 670 nm.  $k_{\text{FNT}}$  = energy transfer rate  $k_{\text{CR}}$  = charge recombination rate constant.

separated state  $\text{ZnP}^+ - \text{ZnPc} - [\text{Cu}(\text{phen})_2]^{2+} - \text{C}_{60}^{\bullet-}$ . Considering the energy of the three different charge separated states relative to the ground state, it must be noted that they exhibit approximately the same energy level (1.31 eV), since the oxidation potentials of  $[\text{Cu}(\text{phen})_2]^+$ ,  $\text{ZnP}$ , and  $\text{ZnPc}$  do not differ appreciably.

**4.3 Rotaxane 3.** Finally, rotaxane 3 was probed with our fs transient absorption setup. The 660 nm fs-excitation exclusively excites ZnPc. Immediately after the laser pulse the ZnPc singlet excited state arises with a maximum at 790 nm and a lifetime of 1.9 ns in THF (800 nm, 1.9 ns in PhCN) (Fig. 13). The singlet excited state decays *via* intersystem crossing (ISC) to the energetically lower lying triplet excited state ( $\sim$ 480 nm), which is stable over the time scale of our experimental setup (7.5 ns). Additionally, ground state bleaching leads to minima at 610 and 680 nm in THF and 615 and 690 nm in PhCN. No clear assignment of transients corresponding to  $\text{C}_{60}^{\bullet-}$ ,  $[\text{Cu}(\text{phen})_2]^+$ , or

any charge separated state could be made in the fs transient absorption experiments, due to their low extinction coefficients and the relatively low energy of the laser excitation (150 nJ). Weak, but broad transient absorptions in the near infrared region (Fig. 13, inset) allows us to conclude that energy transfer occurs to yield the  $^3\text{MLCT}^*$  state.

To gain further insight into the charge transfer dynamics, we turned to longer time scales. Upon ns-excitation (note that in the ns experiment the laser energy is significantly higher than in the fs experiments) of the ZnPc Q-band at 670 nm, the visible region of the differential absorption spectra is dominated by the triplet excited state signature of ZnPc with its maximum at 500 nm, accompanied by ground state bleaching at 610 and 690 nm (Fig. 14, left).<sup>51-57</sup> In the near-infrared region (Fig. 14), the broad  $^3\text{MLCT}^*$  absorption ( $\sim$ 900–1000 nm) is observed. Additionally, two peaks are discernible at 830 and 1020 nm. The former is assigned to  $\text{ZnPc}^+$ , which decays mono-exponentially with a lifetime of  $380 \pm 60$  ns (Fig. 15, left). The peak at 1020 nm corresponds to the one-electron reduced  $\text{C}_{60}^{\bullet-}$  and it is best fit with three exponentials, as seen earlier for rotaxanes 1 and 2 (Fig. 15, center and right). The shortest lifetime of  $88 \pm 9$  ns resembles that found in catenane 8<sup>11,12,18,33</sup> and is ascribed to the  $[\text{Cu}(\text{phen})_2]^+$  centered charge separated state  $\text{Fc-ZnPc} - [\text{Cu}(\text{phen})_2]^{2+} - \text{C}_{60}^{\bullet-}$ . The intermediate lifetime of  $380 \pm 90$  ns matches the lifetime of the one electron oxidized ZnPc and consequently correlates with the ZnPc-centered charge separated state  $\text{Fc-ZnPc}^+ - [\text{Cu}(\text{phen})_2]^+ - \text{C}_{60}^{\bullet-}$ . Finally, the longest lifetime associated with  $\text{C}_{60}^{\bullet-}$  of  $4.9 \pm 0.7$   $\mu$ s is assigned to the thermodynamically most stable long distance charge separated state, namely  $\text{Fc}^+ - \text{ZnPc} - [\text{Cu}(\text{phen})_2]^+ - \text{C}_{60}^{\bullet-}$ . This is consistent with the results obtained for rotaxane 1.

Fig. 16 schematically outlines the excitation and deactivation pathways in rotaxane 3. When exciting directly into the ZnPc Q-bands at 670 nm or into the ZnPc Soret band at 387 nm, the ZnPc singlet excited state is generated, with an energy of 1.83 eV relative to the ground state. Deactivation processes include

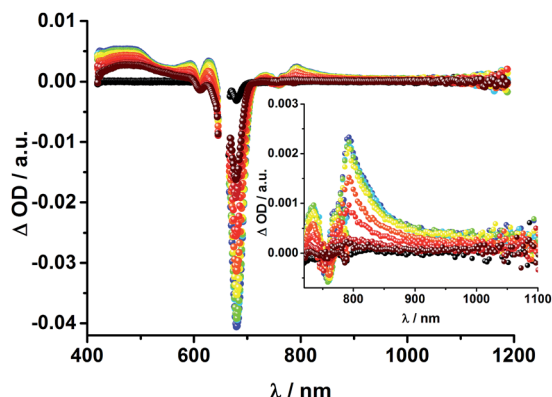


Fig. 13 Transient absorption spectrum (visible and near-infrared) registered upon femtosecond flash photolysis (660 nm, 150 nJ) of  $\text{Fc-ZnPc} - [\text{Cu}(\text{phen})_2]^+ - \text{C}_{60}^{\bullet-}$  rotaxane 3 in THF with time delays between 0 (black) and 5.8 ns (wine) at room temperature. Inset: zoom into the near infrared region.

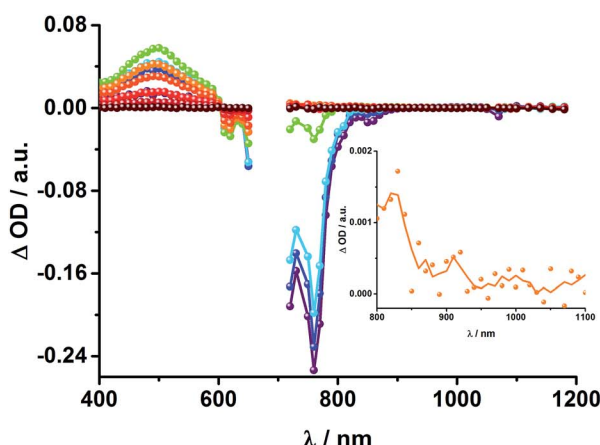
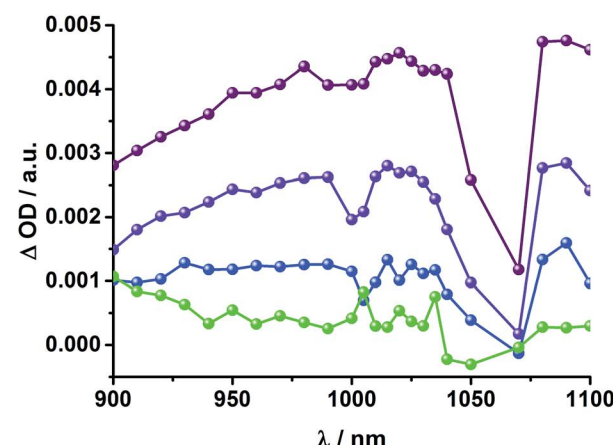


Fig. 14 Left: Differential absorption spectra (visible and near infrared) registered upon nanosecond flash photolysis (670 nm, 5 mJ) of  $\text{Fc-ZnPc} - [\text{Cu}(\text{phen})_2]^+ - \text{C}_{60}^{\bullet-}$  rotaxane 3 under aerobic conditions in THF with time delays between 9 ns (purple) and 2.0  $\mu$ s (wine) at room temperature. Inset: zoom into the near infrared region after 200 ns. Right: Differential absorption spectra (near infrared) registered upon nanosecond flash photolysis (670 nm, 5 mJ) of  $\text{Fc-ZnPc} - [\text{Cu}(\text{phen})_2]^+ - \text{C}_{60}^{\bullet-}$  rotaxane 3 under aerobic conditions in THF with time delays between 9 (purple) and 50 ns (green) at room temperature.



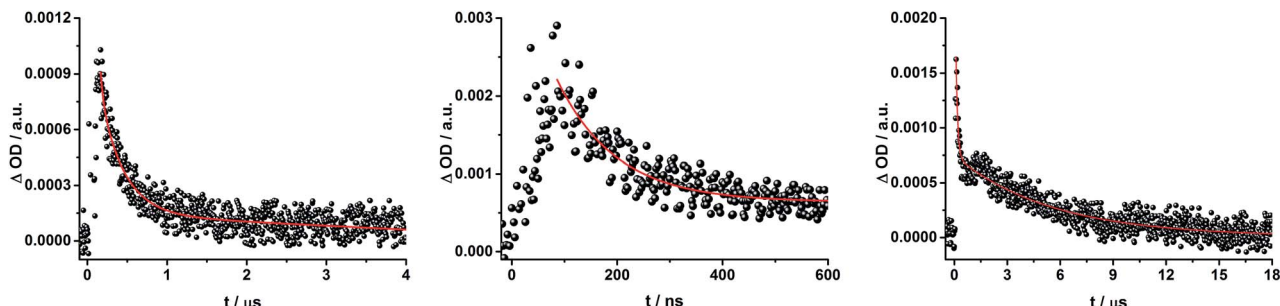


Fig. 15 Time absorption profiles of  $\text{Fc-ZnPc-}[\text{Cu}(\text{phen})_2]^{2+}-\text{C}_60$  rotaxane 3 upon 670 nm excitation in THF at room temperature under aerobic conditions at 830 nm (left) and 1010 nm (center and right), monitoring the charge recombination.

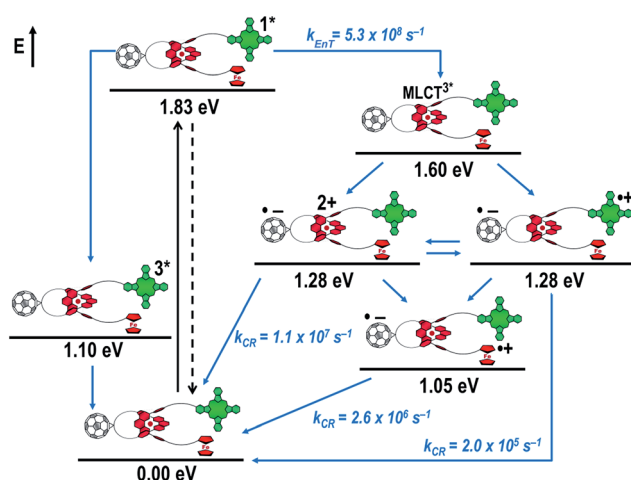


Fig. 16 Schematic energy level diagrams, proposed decay pathways, and rate constants for  $\text{Fc-ZnPc-}[\text{Cu}(\text{phen})_2]^{2+}-\text{C}_60$  rotaxane 3 upon excitation at 670 nm.  $k_{\text{ENT}}$  = energy transfer rate  $k_{\text{CR}}$  = charge recombination rate constant. Energy levels not to scale.

fluorescence with a quantum yield of 15% and ISC to give the triplet excited state of ZnPc ( $\sim 1.1$  eV) followed by the triplet signature in the ns-transient absorption near 500 nm. Deactivation occurs *via* energy transfer to  $[\text{Cu}(\text{phen})_2]^{2+}$ , which is confirmed by 50% quenching of the ZnPc emission (Table S2†). Spectroscopically only the  $^3\text{MLCT}^*$  ( $\sim 1.6$  eV) state can be resolved, since the  $^1\text{MLCT}^*$  is only stable for several hundreds of femtoseconds.<sup>58,59</sup> Electron transfer takes place from the  $^3\text{MLCT}^*$  state to generate the charge separated state  $\text{Fc-ZnPc-}[\text{Cu}(\text{phen})_2]^{2+}-\text{C}_60^{\cdot-}$  with a lifetime of 88 ns ( $k_{\text{CR}} = 1.1 \times 10^7 \text{ s}^{-1}$ ). This state has been identified from the signature absorption of  $\text{C}_60^{\cdot-}$  at 1010 nm (Fig. 14 and 15). Furthermore, two additional lifetimes were found for the  $\text{C}_60^{\cdot-}$ . Thus, we conclude that from the state  $\text{Fc-ZnPc-}[\text{Cu}(\text{phen})_2]^{2+}-\text{C}_60^{\cdot-}$  a charge shift occurs to form the ZnPc- and Fc-centered charge separated states, which are stable for 380 ns ( $k_{\text{CR}} = 2.6 \times 10^6 \text{ s}^{-1}$ ) and 4.9  $\mu\text{s}$  ( $k_{\text{CR}} = 2.0 \times 10^5 \text{ s}^{-1}$ ), respectively. From the present data, it has been impossible to verify with certainty whether the two charge shift processes take place simultaneously or successively. The assignment of the lifetimes from the 1010 nm decay has been made by comparison with  $\text{ZnPc}^{2+}$  decay at  $\sim 830$  nm, and by comparison with the charge separated state lifetimes found for

rotaxanes 1 and 2. Considering the energy levels of the three different charge separated states,  $\text{Fc-ZnPc-}[\text{Cu}(\text{phen})_2]^{2+}-\text{C}_60^{\cdot-}$  and  $\text{Fc-ZnPc}^{2+}-[\text{Cu}(\text{phen})_2]^{2+}-\text{C}_60^{\cdot-}$  seem to exhibit the same energy level, namely 1.28 eV, while the  $\text{Fc}^{2+}-\text{ZnPc-}[\text{Cu}(\text{phen})_2]^{2+}-\text{C}_60^{\cdot-}$  long distance charge separated state at 1.05 eV is thermodynamically most stable.

## Conclusion

It is evident that all three of the newly investigated donor-acceptor rotaxanes undergo similar deactivation pathways upon photoexcitation. The differences become obvious when looking at the charge separated state lifetimes. The  $[\text{Cu}(\text{phen})_2]^{2+}$  centered charge separated states feature lifetimes shorter than 100 ns, while the corresponding ZnPc-centered charge separated state in rotaxanes 2 and 3 exhibit lifetimes in the range of several hundreds of nanoseconds. Although the ZnP centered CS state is energetically at a similar level as those centered at the  $[\text{Cu}(\text{phen})_2]^{2+}$  complex and ZnP ( $\sim 1.3$  eV), considerably longer lifetimes (in the microsecond time regime) are observed for the former. In case of the  $[\text{Cu}(\text{phen})_2]^{2+}$ -centered charge separated state, the shorter lifetimes arise from shorter distances between the radical ions, while ZnPc is generally known to form shorter lived radical ion pairs with  $\text{C}_60$  than ZnP, since smaller energy gaps for the back electron transfer step pulls these processes closer to the top of the Marcus parabola.<sup>1,60</sup> The longest lifetimes determined are for the energetically favored Fc-centered charge separated state ( $\sim 1.1$  eV). However, in rotaxane 1, the lifetime (61  $\mu\text{s}$ ) is considerably longer than for rotaxane 3 (4.9  $\mu\text{s}$ ). Thus, it is concluded that the  $\text{Fc}^{2+}-\text{C}_60^{\cdot-}$  charge separated state is better stabilized by ZnP (rotaxane 1) than by ZnPc (rotaxane 3).

In comparison to previously studied rotaxanes incorporating either ZnPc,<sup>61</sup> Fc,<sup>16</sup> or ZnP,<sup>14,15,18</sup> significantly longer charge separated state lifetimes have been achieved in the new rotaxanes 1, 2, and 3. For example, in ferrocene stoppered  $[\text{Cu}(\text{phen})_2]^{2+}-\text{C}_60$  rotaxanes only the  $(\text{Fc})_2-[\text{Cu}(\text{phen})_2]^{2+}-\text{C}_60^{\cdot-}$  charge separated state with a lifetime of 15–16 ns ( $k_{\text{CR}} = 6.3$  to  $6.7 \times 10^7 \text{ s}^{-1}$ ) was observed, without any appreciable evidence for a subsequent charge shift to the ferrocene units.<sup>16</sup> However, when replacing one of the Fc stoppers by ZnP (rotaxane 1) or ZnPc (rotaxane 3), a charge shift from ZnP and ZnPc to the



ferrocene takes place to yield the thermodynamically most stable Fc-centered charge separated states, with lifetimes in the microsecond regime. In our previously reported  $C_{60}$ -stoppered porphyrino-rotaxanes, a long lived  $ZnP^{*+}-[Cu(phen)_2]^+-(C_{60})_2^{*-}$  of  $32\ \mu s$  lifetime ( $k_{CR} = 3.1 \times 10^4\ s^{-1}$ ) were detected.<sup>14</sup> However, when combining the virtues of ZnP and Fc as electron donors, as in the present work, charge separated states with almost twice that lifetime are achievable. Therefore, the combination in a single  $[Cu(phen)_2]^+$ -based rotaxane system of the outstanding electrochemical and spectroscopic properties of ZnP with the low oxidation potential of ferrocene and the extraordinary electron accepting properties and low reorganization energy of  $C_{60}$  yields very attractive photoactive materials, which are capable of absorbing light over a very wide range of the visible spectrum and undergoing a cascade of energy and electron transfer processes that ultimately produce charge separated states with lifetimes in the microsecond time domain, as high as  $61\ \mu s$ .

## Acknowledgements

This work was funded by Solar Technologies go Hybrid.

## Notes and references

- 1 S. Kirner, M. Sekita and D. M. Guldì, *Adv. Mater.*, 2014, **26**, 1482–1493.
- 2 P. L. Anelli, P. R. Ashton, R. Ballardini, V. Balzani, M. Delgado, M. T. Gandolfi, T. T. Goodnow, A. E. Kaifer, D. Philp, P. Marek, L. Prodi, M. V. Reddington, A. M. Z. Slawin, N. Spencer, J. F. Stoddart, C. Vicent and D. J. Williams, *J. Am. Chem. Soc.*, 1992, **114**, 193–218.
- 3 P. R. Ashton, V. Balzani, A. Credi, O. Kocian, D. Pasini, L. Prodi, N. Spencer, J. F. Stoddart, M. S. Tolley, M. Venturi, A. J. P. White and D. J. Williams, *Chem.-Eur. J.*, 1998, **4**, 590–607.
- 4 P. R. Ashton, T. T. Goodnow, A. E. Kaifer, M. V. Reddington, A. M. Z. Slawin, N. Spencer, J. F. Stoddart, C. Vicent and D. J. Williams, *Angew. Chem., Int. Ed.*, 1989, **28**, 1396–1399.
- 5 J. D. Megiatto Jr, A. Antoniuk-Pablant, B. D. Sherman, G. Kodis, M. Gervaldo, T. A. Moore, A. L. Moore and D. Gust, *Proc. Natl. Acad. Sci. U. S. A.*, 2012, **109**, 15578–15583.
- 6 J. D. Megiatto Jr, D. D. Mendez-Hernandez, M. E. Tejeda-Ferrari, A. L. Teillout, M. J. Llansola-Portoles, G. Kodis, O. G. Poluektov, T. Rajh, V. Mujica, T. L. Groy, D. Gust, T. A. Moore and A. L. Moore, *Nat. Chem.*, 2014, **6**, 423–428.
- 7 Y. Zhao, J. R. Swierk, J. D. Megiatto Jr, B. Sherman, W. J. Youngblood, D. Qin, D. M. Lentz, A. L. Moore, T. A. Moore, D. Gust and T. E. Mallouk, *Proc. Natl. Acad. Sci. U. S. A.*, 2012, **109**, 15612–15616.
- 8 L. Kálmán, R. LoBrutto, J. P. Allen and J. C. Williams, *Nature*, 1999, **402**, 696–699.
- 9 X. Lin, H. A. Murchison, V. Nagarajan, W. W. Parson, J. P. Allen and J. C. Williams, *Proc. Natl. Acad. Sci. U. S. A.*, 1994, **91**, 10265–10269.
- 10 P. L. Dutton and C. C. Mosser, *Proc. Natl. Acad. Sci. U. S. A.*, 1994, **91**, 10247–10250.
- 11 J. D. Megiatto Jr, D. I. Schuster, S. Abwandner, G. de Miguel and D. M. Guldì, *J. Am. Chem. Soc.*, 2010, **132**, 3847–3861.
- 12 J. D. Megiatto Jr, D. I. Schuster, G. de Miguel, S. Wolfrum and D. M. Guldì, *Chem. Mater.*, 2012, **24**, 2472–2485.
- 13 J. D. Megiatto Jr, R. Spencer and D. I. Schuster, *J. Mater. Chem.*, 2011, **21**, 1544.
- 14 K. Li, P. J. Bracher, D. M. Guldì, M. A. Herranz, L. Echegoyen and D. I. Schuster, *J. Am. Chem. Soc.*, 2004, **126**, 9156–9157.
- 15 K. Li, D. I. Schuster, D. M. Guldì, M. A. Herranz and L. Echegoyen, *J. Am. Chem. Soc.*, 2004, **126**, 3388–3389.
- 16 J. D. Megiatto Jr, K. Li, D. I. Schuster, A. Palkar, M. A. Herranz, L. Echegoyen, S. Abwandner, G. Miguel and D. M. Guldì, *J. Phys. Chem. B*, 2010, **114**, 14408–14419.
- 17 J. D. Megiatto Jr, R. Spencer and D. I. Schuster, *Org. Lett.*, 2009, **11**, 4152–4155.
- 18 D. I. Schuster, K. Li, D. M. Guldì and J. Ramey, *Org. Lett.*, 2004, **6**, 1919–1922.
- 19 L. Flamigni, A. M. Talarico, J. C. Chambron, V. Heitz, M. Linke, N. Fujita and J. P. Sauvage, *Chem.-Eur. J.*, 2004, **10**, 2689–2699.
- 20 C. O. Dietrich-Buchecker and J.-P. Sauvage, *Tetrahedron Lett.*, 1983, **24**, 5095–5098.
- 21 C. O. Dietrich-Buchecker and J.-P. Sauvage, *J. Am. Chem. Soc.*, 1984, **106**, 3043–3045.
- 22 C. O. Dietrich-Buchecker and J.-P. Sauvage, *Chem. Rev.*, 1987, **87**, 795–810.
- 23 C. O. Dietrich-Buchecker and J.-P. Sauvage, *Tetrahedron*, 1990, **46**, 503–512.
- 24 J.-P. Sauvage and C. O. Dietrich-Buchecker, *Molecular Catenanes, Rotaxanes and Knots*, Wiley VCH, Weinheim, Germany, 1999.
- 25 J. D. Megiatto Jr and D. I. Schuster, *Org. Lett.*, 2011, **13**, 1808–1811.
- 26 M. Andersson, M. Linke, J.-C. Chambron, J. Davidsson, V. Heitz, J.-P. Sauvage and L. Hammarström, *J. Am. Chem. Soc.*, 2000, **122**, 3526–3527.
- 27 M. Linke, J.-C. Chambron, V. Heitz and J.-P. Sauvage, *J. Am. Chem. Soc.*, 1997, **119**, 11329–11330.
- 28 J. S. Lindsey, *Acc. Chem. Res.*, 2010, **43**, 300–311.
- 29 E. M. Maya, P. Vázquez and T. Torres, *Chem. - Eur. J.*, 1999, **5**, 2004–2013.
- 30 J. D. Megiatto Jr and D. I. Schuster, *Chem. - Eur. J.*, 2009, **15**, 5444–5448.
- 31 J. P. C. Tomé, A. M. V. M. Pereira, C. M. A. Alonso, M. G. P. M. S. Neves, A. C. Tomé, A. M. S. Silva, J. A. S. Cavaleiro, M. V. Martínez-Díaz, T. Torres, G. M. A. Rahman, J. Ramey and D. M. Guldì, *Eur. J. Org. Chem.*, 2006, **1**, 257–267.
- 32 S. FitzGerald, C. Farren, C. F. Stanley, A. Beeby and M. R. Bryce, *Photochem. Photobiol. Sci.*, 2002, **1**, 581–587.
- 33 S. V. Kirner, D. M. Guldì, J. D. Megiatto Jr and D. I. Schuster, *Nanoscale*, 2015, **7**, 1145–1160.
- 34 T. Kato, T. Kodama, T. Shida, T. Nakagawa, Y. Matsui, S. Suzuki, H. Shiromaru, K. Yamauchi and Y. Achiba, *Chem. Phys. Lett.*, 1991, **180**, 446–450.



35 S. A. Vail, P. J. Krawczuk, D. M. Guldi, A. Palkar, L. Echegoyen, J. P. C. Tome, M. A. Fazio and D. I. Schuster, *Chem.-Eur. J.*, 2005, **11**, 3375–3388.

36 L. Pekkarinen and H. Linschitz, *J. Am. Chem. Soc.*, 1960, **82**, 2407–2411.

37 T. Kato, *Laser Chem.*, 1994, **14**, 155–160.

38 D. M. Guldi, M. Maggini, G. Scorrano and M. Prato, *J. Am. Chem. Soc.*, 1997, **119**, 974–980.

39 H. Imahori, H. Norieda, H. Yamada, Y. Nishimura, I. Yamazaki, Y. Sakata and S. Fukuzumi, *J. Am. Chem. Soc.*, 2001, **123**, 100–110.

40 H. Imahori, K. Tamaki, D. M. Guldi, C. Luo, M. Fujitsuka, O. Ito, Y. Sakata and S. Fukuzumi, *J. Am. Chem. Soc.*, 2001, **123**, 2607–2617.

41 H. Imahori, H. Yamada, Y. Nishimura, I. Yamazaki and Y. Sakata, *J. Phys. Chem. B*, 2000, **104**, 2099–2108.

42 F. Spanig, C. Kovacs, F. Hauke, K. Ohkubo, S. Fukuzumi, D. M. Guldi and A. Hirsch, *J. Am. Chem. Soc.*, 2009, **131**, 8180–8195.

43 D. Gonzalez-Rodriguez, T. Torres, M. M. Olmstead, J. Rivera, M. A. Herranz, L. Echegoyen, C. A. Castellanos and D. M. Guldi, *J. Am. Chem. Soc.*, 2006, **128**, 10680–10681.

44 D. M. Guldi, *Chem. Soc. Rev.*, 2002, **31**, 22–36.

45 C. Grewer and H.-D. Brauer, *J. Phys. Chem.*, 1994, **98**, 4230–4235.

46 R. A. Marcus, *Angew. Chem.*, 1993, **105**, 1161–1172.

47 G. Grampp, *Angew. Chem., Int. Ed.*, 1993, **32**, 691–693.

48 D. M. Guldi, *Chem. Commun.*, 2000, 321–327.

49 C. Luo, D. M. Guldi, H. Imahori, K. Tamaki and Y. Sakata, *J. Am. Chem. Soc.*, 2000, **122**, 6535–6551.

50 D. M. Guldi, A. Gouloumis, P. Vázquez and T. Torres, *Chem. Commun.*, 2002, 2056–2057.

51 A. Hausmann, A. R. Soares, M. V. Martinez-Díaz, M. G. Neves, A. C. Tome, J. A. Cavaleiro, T. Torres and D. M. Guldi, *Photochem. Photobiol. Sci.*, 2010, **9**, 1027–1032.

52 A. M. V. M. Pereira, A. R. M. Soares, A. Hausmann, M. G. P. M. S. Neves, A. C. Tomé, A. M. S. Silva, J. A. S. Cavaleiro, D. M. Guldi and T. Torres, *Phys. Chem. Chem. Phys.*, 2011, **13**, 11858.

53 M. Quintiliani, A. Kahnt, T. Wolfle, W. Hieringer, P. Vazquez, A. Gorling, D. M. Guldi and T. Torres, *Chem.-Eur. J.*, 2008, **14**, 3765–3775.

54 W. Seitz, A. Kahnt, D. M. Guldi and T. Torres, *J. Porphyrins Phthalocyanines*, 2009, **13**, 1034–1039.

55 R. F. Enes, J. J. Cid, A. Hausmann, O. Trukhina, A. Gouloumis, P. Vazquez, J. A. Cavaleiro, A. C. Tome, D. M. Guldi and T. Torres, *Chem.-Eur. J.*, 2012, **18**, 1727–1736.

56 A. J. Jimenez, M. L. Marcos, A. Hausmann, M. S. Rodriguez-Morgade, D. M. Guldi and T. Torres, *Chem.-Eur. J.*, 2011, **17**, 14139–14146.

57 A. M. Pereira, A. Hausmann, A. R. Soares, J. P. Tome, O. Trukhina, M. Urbani, M. G. Neves, J. A. Cavaleiro, D. M. Guldi and T. Torres, *Chem.-Eur. J.*, 2012, **18**, 3210–3219.

58 N. Armaroli, M. A. J. Rodgers, P. Ceroni, V. Balzani, C. O. Dietrich-Buchecker, J.-M. Kern, A. Bailal and J.-P. Sauvage, *Chem. Phys. Lett.*, 1995, **241**, 555–558.

59 T. Gunaratne, M. A. J. Rodgers, D. Felder, J.-F. Nierengarten, G. Accorsi and N. Armaroli, *Chem. Commun.*, 2003, 3010.

60 G. Bottari, G. de la Torre, D. M. Guldi and T. Torres, *Chem. Rev.*, 2010, **110**, 6768–6816.

61 D. M. Guldi, J. Ramey, M. V. Martínez-Díaz, A. de la Escosura, T. Torres, T. da Ros and M. Prato, *Chem. Commun.*, 2002, 2774–2775.

